Decay of one dimensional surface modulations

Navot Israeli* and Daniel Kandel**
Department of Physics of Complex Systems,
Weizmann Institute of Science, Rehovot 76100, Israel

The relaxation process of one dimensional surface modulations is re-examined. Surface evolution is described in terms of a standard step flow model. Numerical evidence that the surface slope, $D(x,t)$, obeys the scaling ansatz $D(x,t) = \alpha(t)F(x)$ is provided. We use the scaling ansatz to transform the discrete step model into a continuum model for surface dynamics. The model consists of differential equations for the functions $\alpha(t)$ and $F(x)$. The solutions of these equations agree with simulation results of the discrete step model. We identify two types of possible scaling solutions. Solutions of the first type have facets at the extremum points, while in solutions of the second type the facets are replaced by cusps. Interactions between steps of opposite signs determine whether a system is of the first or second type. Finally, we relate our model to an actual experiment and find good agreement between a measured AFM snapshot and a solution of our continuum model.

68.55.-a, 68.35.Bs

I. INTRODUCTION

Periodic crystalline surfaces are a convenient testing ground for modeling surface evolution and considerable efforts have been devoted to their study. The decay of one and two dimensional surface modulations has been investigated extensively. The emerging experimental picture is that above the roughening transition temperature, T_R, such structures decay as pure sine waves[1]. This fact is well explained by Mullins' theory[2] which treats the surface as an isotropic object. However, below T_R the situation is different and one must take into account the anisotropy of the underlying crystal lattice. This anisotropy produces cusp singularities in the crystal surface tension at high symmetry planes, which lead to the formation of facets[1,3–6].

From the theoretical point of view, the existence of cusps in the surface tension complicates the description of surface evolution in terms of continuous models. Such models usually assume that mass transfer follows gradients in the *continuous* surface chemical potential. However, the chemical potential is singular at facet edges and the dynamics in the vicinity of these regions must be treated with special care.

There are basically two ways to deal with the above problem. The first one is to avoid it all together by resorting to microscopic models. Step flow models[7–9] and Monte Carlo simulations[10–15] describe surface dynamics in terms of *discrete* microscopic objects. On this level the surface chemical potential is no longer continuous and there are no singularity problems. Facets are natural phenomena in such a framework. However in going to microscopic models one usually loses the mathematical simplicity of the continuum approach. Step flow models and Monte Carlo simulations are usually solved numerically and it is difficult to derive the large scale dynamics from them.

The second way is to use continuum models in which singular points are treated as moving[16] or stationary[7] boundaries. Alternatively, surface tension singularities can be smoothed out[17,18] assuming that if smoothing is done on a small length scale the large scale results will not be affected. The drawback of these continuum approaches is that by starting with a continuum model one loses sight of the underlying microscopic kinetics. As pointed out by Chame et al.[19], the connection of these models with the details of the microscopic processes is unclear. We show below that these details are important and may lead to large scale effects.

In this work we re-examine the relaxation process of unidirectional surface modulations. Our aim is to derive a continuum model for the surface evolution which is consistent with

the microscopic kinetics. We adopt here the same approach we used in the study of other surface structures[20–22]. First we study the system's behavior in terms of a standard step flow model. The model allows steps of opposite sign to interact; such interactions can lead to facet formation. Numerical simulations of the step model suggest that the surface slope $D(x,t)$ follows the simple scaling law $D(x,t) = \alpha(t)F(x)$. The derivation of the step model and its numerical analysis are carried out in Section II. In Section III we use the scaling ansatz to transform the step flow model into a continuum model, i.e., we derive the differential equations for the functions $\alpha(t)$ and $F(x)$ directly from the step velocities of the discrete model. In Section IV we solve the resulting differential equations and find the scaling function F. We find an impressive agreement between this scaling function and simulations of the step model.

In Section V we discuss the relevance of our model to AFM measurements of decaying surface modulations taken by Tanaka et al.[3]. We show that the best fit solution of our model agrees with the experimental data. On this basis we derive a formula which connects microscopic parameters in the system with the measured life time of the profile. Our conclusions and their relation to existing work are presented in section VI.

II. STEP FLOW MODEL OF 1D MODULATIONS

Consider a 1D grating of wavelength λ fabricated on a high symmetry crystal orientation as illustrated in Fig. 1. Below the roughening transition one can ignore the existence of islands and voids and describe the surface as consisting of flat terraces separated by straight atomic steps. In the absence of evaporation and when no new material is added, these steps move by mass exchange with the adatom diffusion fields on neighboring terraces. Such evolution was treated in the spirit of the Burton-Cabrera-Frank model[23] by a number of authors. In what follows we use a standard step model for surface evolution. This model is essentially equivalent to the one used by Ozdemir and Zangwill in Ref. 7 except that we allow steps of opposite sign to interact. For completeness we now derive the model.

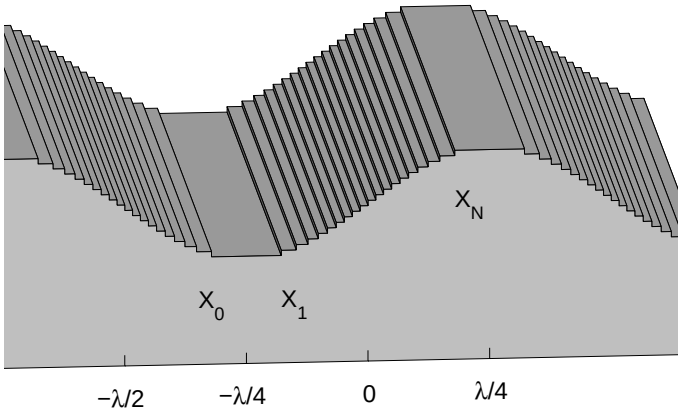

FIG. 1. Illustration of a modulated surface below the roughening transition. The step labeling is indicated. We label the terraces such that the nth terrace separates the nth and $n+1$th steps.

To describe step motion mathematically, one has to solve the adatom diffusion problem on the terraces. Let us denote the adatom concentration field on the nth terrace by $C_n(x)$. In most situations, the time scale associated with step motion is much larger than the time scale of surface diffusion. One can therefore assume that the adatom concentration field is always in a steady state; i.e, for any given step configuration, $C_n(x)$ reaches a steady state

before the steps move significantly. Within this quasi-static approximation $C_n(x)$ obeys the static diffusion equation $\nabla^2 C_n(x) = 0$, which is readily solved by

$$C_n(x) = a_n + b_n x \ . \tag{1}$$

Next we look at the boundary conditions for these diffusion fields. Near the step edges the diffusion currents are determined by the flux of atoms emitted or absorbed by the steps. Assuming linear kinetics characterized by an attachment-detachment rate k, the current of atoms on both sides of the nth step is given by[24]

$$\begin{aligned} J_{n-1} &= -D_s \nabla C_{n-1}(x_n) = k\left[C_{n-1}(x_n) - C_n^{eq}\right] \ , \\ J_n &= -D_s \nabla C_n(x_n) = -k\left[C_n(x_n) - C_n^{eq}\right] \ . \end{aligned} \tag{2}$$

Here D_s is the adatom diffusion coefficient, x_n is the position of the nth step, J_n is the current across the nth terrace and C_n^{eq} is the equilibrium adatom concentration at x_n.

Eqs. (1) and (2) can be used to calculate the constants a_n and b_n and thus fully determine the adatom concentration fields. We find that

$$J_n = -D_s b_n = \frac{D_s\left(C_n^{eq} - C_{n+1}^{eq}\right)}{\frac{2D_s}{k} + x_{n+1} - x_n} \ . \tag{3}$$

Mass conservation implies that the velocity of the nth step takes the form

$$\frac{dx_n}{dt} = \Omega\left(J_n - J_{n-1}\right) \ , \tag{4}$$

where Ω is the atomic area of the solid.

In order to complete the model, we write down expressions for C_n^{eq}. To this end we introduce the step chemical potential μ_n, which is associated with the addition of an atom to the solid at the nth step. C_n^{eq} depends on the step chemical potential in the following way:

$$C_n^{eq} = \tilde{C}^{eq} \exp\frac{\mu_n}{k_B T} \approx \tilde{C}^{eq}\left(1 + \frac{\mu_n}{k_B T}\right) \ . \tag{5}$$

$\tilde{C}^{eq}$ is the equilibrium concentration of a noninteracting step, k_B is the Boltzmann constant and T is the temperature.

Finally, to evaluate μ_n we take into account repulsive interactions with strength $\beta/2$ between nearest neighbor steps of the same sign:

$$U(x_n, x_{n+1}) = \frac{\beta}{2\left(x_{n+1} - x_n\right)^2}. \tag{6}$$

Such a repulsion is consistent with entropic as well as elastic[25,26] interactions between straight steps. We also take into account the possibility of an attractive interaction with strength $\tilde{\beta}/2$ between nearest neighbor steps of opposite signs:

$$\tilde{U}(x_n, x_{n+1}) = -\frac{\tilde{\beta}}{2\left(x_{n+1} - x_n\right)^2}. \tag{7}$$

An elastic attraction of this form may exist in some materials[25]. In addition, step-antistep annihilation events are accelerated by step fluctuations[9,19]. In our one dimensional model, step fluctuations are not treated. Instead, this kinetic effect can be introduced as an effective

step-antistep attraction. Although the form of this kinetic attraction may be different, Eq. (7) can be viewed as a phenomenological ingredient of our model which enables us to study the effect of step-antistep attraction on surface evolution. Using the above interactions the chemical potentials of steps $1,\ldots,N$ in Fig. 1 are given by

$$\begin{aligned}
\mu_1 &= \frac{\partial\left[\tilde{U}\left(x_0,x_1\right)+U\left(x_1,x_2\right)\right]}{\partial x_1} = \frac{\beta}{\left(x_2-x_1\right)^3}+\frac{\tilde{\beta}}{\left(x_1-x_0\right)^3}\ , \\
\mu_n &= \frac{\partial\left[U\left(x_{n-1},x_n\right)+U\left(x_n,x_{n+1}\right)\right]}{\partial x_n} = \frac{\beta}{\left(x_{n+1}-x_n\right)^3}-\frac{\beta}{\left(x_n-x_{n-1}\right)^3}, \quad n=2,\ldots,N-1, \\
\mu_N &= \frac{\partial\left[U\left(x_{N-1},x_N\right)+\tilde{U}\left(x_N,x_{N+1}\right)\right]}{\partial x_N} = -\frac{\beta}{\left(x_N-x_{N-1}\right)^3}-\frac{\tilde{\beta}}{\left(x_{N+1}-x_N\right)^3}\ . \qquad (8)
\end{aligned}$$

Eqs. (3), (4), (5) and (8) constitute a complete model for surface evolution. This model depends on six parameters but many of them are trivial. The only non trivial parameters in the model are the ratio $g=\tilde{\beta}/\beta$, which measures the relative strength of the two interactions, and the length $l=\frac{2D_s}{k}$. The latter determines the rate limiting process in the system. When $l\to 0$ attachment-detachment events are relatively fast and the kinetics is diffusion limited (DL). In the opposite case, $l\to\infty$, diffusion is relatively fast and the kinetics is attachment-detachment limited (ADL). The combined effect of all the other parameters can be scaled out by transforming to dimensionless variables. In the DL case we choose

$$\begin{aligned}
\tilde{x} &= \frac{2\pi}{\lambda}x\ , \\
\tilde{t} &= \left(\frac{\lambda}{2\pi}\right)^5\cdot\frac{k_BT}{\Omega D_s\tilde{C}^{eq}\beta}t\ . \qquad (9)
\end{aligned}$$

In all other non-diffusion-limited (NDL) cases we choose

$$\tilde{t} = \left(\frac{\lambda}{2\pi}\right)^4\cdot\frac{k_BT}{\Omega k\tilde{C}^{eq}\beta}t\ . \qquad (10)$$

with the same definition of $\tilde{x}$. In the remainder of this section we study surface evolution through numerical simulations of the above model in terms of the dimensionless variables $\tilde{x}$ and $\tilde{t}$.

Figure 2 presents the simulation results of a typical system. We show a plot of the step configuration in one wave length of the profile. The initial step configuration corresponds to a sinusoidal surface profile. After a short transient step-antistep pairs at the top and bottom terraces start annihilating. As a result, the steps in the sloping parts of the profile become less densed.

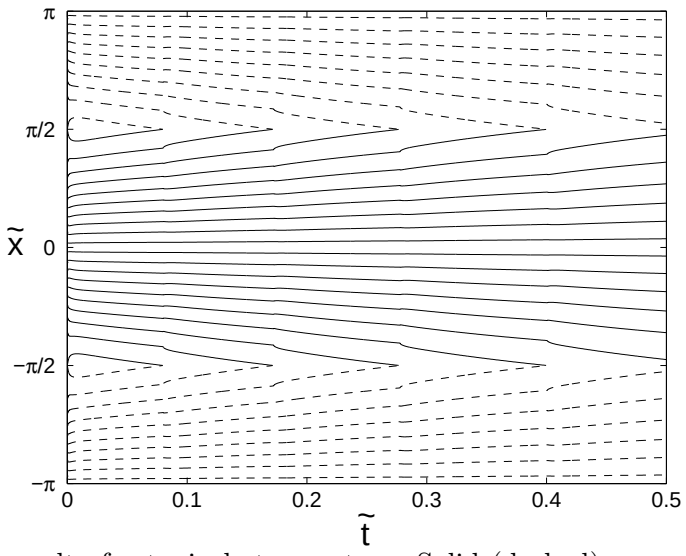

FIG. 2. Simulation result of a typical step system. Solid (dashed) curves show the position of steps (antisteps). Steps and antisteps collide and annihilate at the profile maximum ($\tilde{x} = \pi/2$) and minimum ($\tilde{x} = -\pi/2$).

To further understand the surface evolution let us study step kinetics through their density function (the profile slope). We define the step density between two neighboring steps of the same sign as the inverse step separation, i.e.,

$$D\left(\frac{\tilde{x}_{n+1} + \tilde{x}_n}{2}, \tilde{t}\right) = \pm \frac{1}{\tilde{x}_{n+1}(\tilde{t}) - \tilde{x}_n(\tilde{t})} \ , \tag{11}$$

where the $\pm$ signs distinguish between steps and antisteps. The density between two steps of opposite sign is defined to be zero, consistently with the profile slope.

$D(\tilde{x}, \tilde{t})$ is a continuous function of $\tilde{t}$, defined at a discrete set of positions at any given time. It turns out that the evolution of this function obeys a simple scaling ansatz. When we scale the step density to unity at its peak and then plot density functions from different times, all the data collapses onto a single curve. In other words, there exist functions $F(\tilde{x})$ and $\alpha(\tilde{t}) = \max_{\{\tilde{x}\}} D(\tilde{x}, \tilde{t})$, which satisfy the relation

$$D\left(\tilde{x}, \tilde{t}\right) = \alpha\left(\tilde{t}\right) F\left(\tilde{x}\right) \ , \tag{12}$$

for every $\tilde{x} = \left(\tilde{x}_{n+1} + \tilde{x}_n\right)/2$. Note that since the step positions vary continuously with time, F is a function of a *continuous* variable.

Figure 3 demonstrates the data collapse obtained when the density function is divided by its amplitude, $\alpha(\tilde{t})$, at different times for the ADL case with (Fig. 3a) and without (Fig. 3b) step-antistep attraction. Only half a period of a profile modulation is shown, since by symmetry the density of antisteps in the other half behaves in exactly the same way. A similar behavior is seen in the DL limit. We note that in all cases the system exhibits scaling to a good approximation, but the quality of the data collapse is slightly better in the cases without step-antistep attraction ($g = 0$). The second observation is that when step-antistep attraction is present, the scaling function is steeper and has a smaller step density near the profile extrema. This is a result of the faster step-antistep annihilation process due to the attraction.

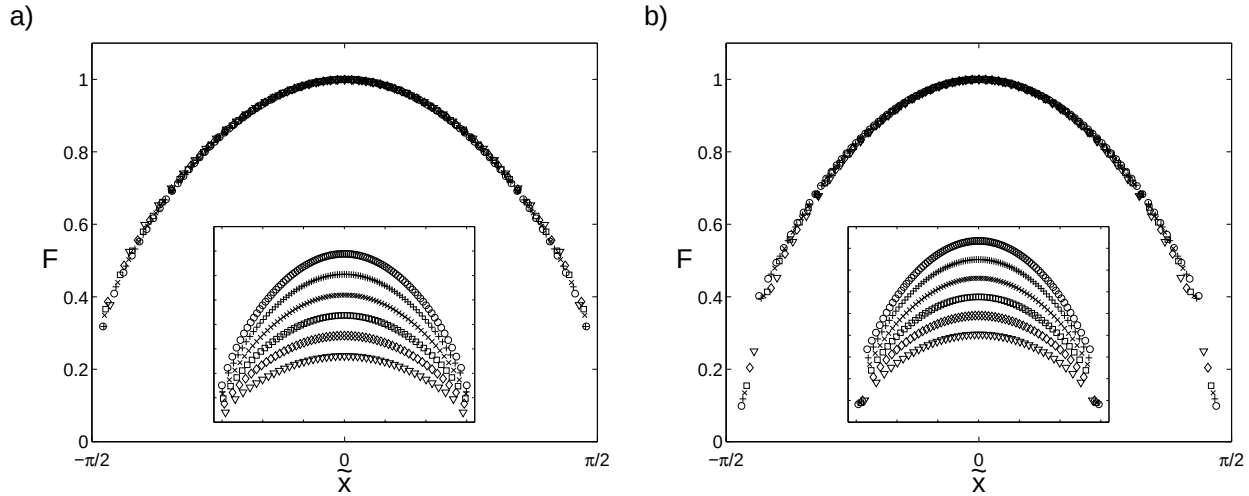

FIG. 3. Data collapse of density functions in the ADL case with a) $g = 0$ and b) $g = 24$. Note that in the presence of step-antistep attraction ($g = 24$) the density function is steeper and has a smaller value near the profile extrema.

While there is no significant difference between the ADL and DL scaling functions, the time dependent amplitude, $\alpha(\tilde{t})$, does show different behaviors. In Fig. 4 we plot $\alpha(\tilde{t})$ for ADL and DL systems, with and without step-antistep attraction. In the ADL cases, $\alpha(\tilde{t})$ can be fitted by an exponential decay, while in the DL cases $\alpha(\tilde{t}) \sim (\tilde{t} - \tilde{t}_0)^{-1}$ consistently with Ref. 7.

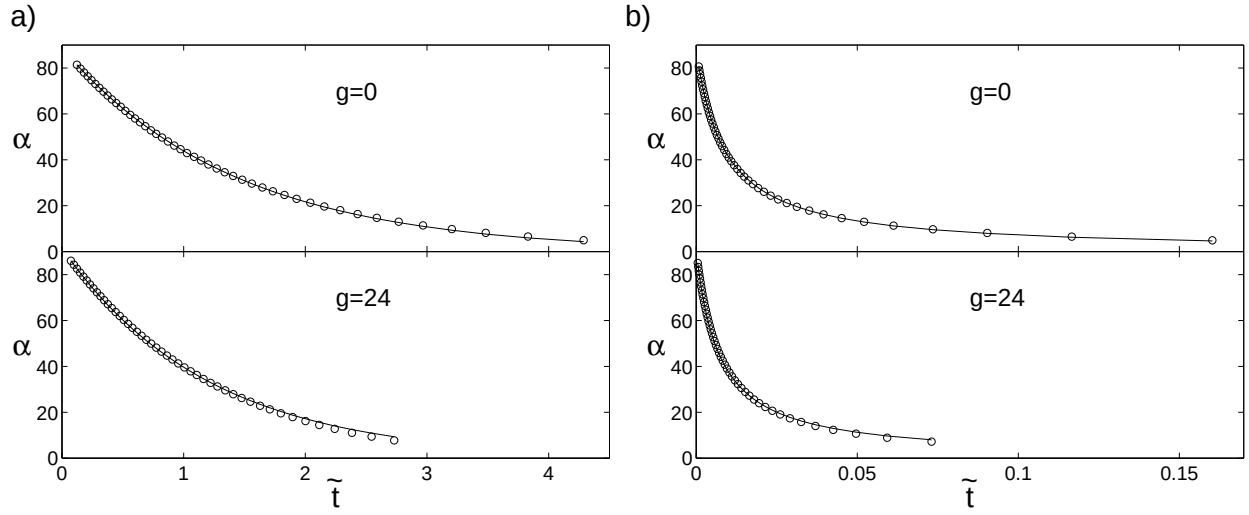

FIG. 4. The amplitudes $\alpha(\tilde{t})$ in different systems (circles): a) ADL with $g = 0$ and $g = 24$, b) DL with $g = 0$ and $g = 24$. In the ADL cases the amplitudes can be fitted (solid lines in a) by $\alpha = A * e^{-\tilde{t}/\tau}$ with $\tau = 1.42$ for the $g = 0$ case and $\tau = 1.196$ for the $g = 24$ case. In the DL cases the amplitudes can be fitted (solid lines in b) by $\alpha = \tau/(\tilde{t} - \tilde{t}_0)$ with $\tau = 0.785$ for the $g = 0$ case and $\tau = 0.643$ for the $g = 24$ case. Note that in the presence of step-antistep attraction the decay is faster.

III. SCALING ANALYSIS AND A CONTINUUM MODEL

The simulation results from the previous section suggest that the step density in the discrete step model can be described by the continuous functions $\alpha(\tilde{t})$ and $F(\tilde{x})$. This

situation is similar in many aspects to the one encountered in a different step system which describes the decay of a crystalline cone[20,21]. Although the cone system obeys a different scaling scenario, we use here the same scaling analysis, described in detail in Ref. 21. Our aim is to derive the differential equations for the functions $\alpha(\tilde{t})$ and $F(\tilde{x})$.

Assuming that the scaling ansatz (12) indeed holds, we write the full time derivative of the step density:

$$\frac{dD}{d\tilde{t}} = \frac{\partial D}{\partial \tilde{t}} + \frac{\partial D}{\partial \tilde{x}} \cdot \frac{d\tilde{x}}{d\tilde{t}} \; . \tag{13}$$

Equation (13) can be evaluated in the middle of the terrace between two steps, i.e. at $\tilde{x} = (\tilde{x}_n + \tilde{x}_{n+1})/2$. The time derivative of $\tilde{x}$ is then given by $d\tilde{x}/d\tilde{t} = (\dot{\tilde{x}}_n + \dot{\tilde{x}}_{n+1})/2$ where $\dot{\tilde{x}}_n \equiv d\tilde{x}_n/d\tilde{t}$. The l.h.s. of Eq. (13) can be calculated by taking the time derivative of Eq. (11): $dD/d\tilde{t} = -D^2\left(\dot{\tilde{x}}_{n+1} - \dot{\tilde{x}}_n\right)$. Using the scaling ansatz, (12), we express Eq. (13) in terms of the functions $\alpha(\tilde{t})$ and $F(\tilde{x})$:

$$\alpha F' \frac{\dot{\tilde{x}}_{n+1} + \dot{\tilde{x}}_n}{2} + \dot{\alpha} F + \alpha^2 F^2 \left(\dot{\tilde{x}}_{n+1} - \dot{\tilde{x}}_n\right) = 0 \; . \tag{14}$$

$\dot{\alpha}$ and F' are the $\tilde{t}$ and $\tilde{x}$ derivatives of α and F, respectively. The step velocities $\dot{\tilde{x}}_n$ and $\dot{\tilde{x}}_{n+1}$ can in principle be expressed in terms of the $\tilde{x}_n$'s using Eq. (4), but we defer this manipulation to a later stage.

Let us also rewrite Eq. (11) in terms of α and F:

$$\tilde{x}_{n+1} - \tilde{x}_n = \frac{1}{\alpha F\left[(\tilde{x}_{n+1} + \tilde{x}_n)/2\right]} \; . \tag{15}$$

According to this, the difference between successive $\tilde{x}_n$'s is of order α^{-1} wherever F does not vanish. This allows us to expand Eq. (14) in powers of α^{-1} when α is large and the step density is high. We can consider only the leading order in α^{-1}, an approximation which becomes exact in the scaling limit $\alpha \to \infty$. The differences $\tilde{x}_{n+k} - \tilde{x}$, where $\tilde{x}$ denotes the middle of the terrace, are also small as long as k is finite. This allows us to go to a continuum limit in the variable $\tilde{x}$ in the following way. We evaluate the function F at the position $(\tilde{x}_{n+k} + \tilde{x}_{n+k+1})/2$ by using its Taylor expansion

$$F\left(\frac{\tilde{x}_{n+k} + \tilde{x}_{n+k+1}}{2}\right) \equiv \frac{\alpha^{-1}}{\tilde{x}_{n+k+1} - \tilde{x}_{n+k}} = \sum_{m=0}^{\infty} \frac{1}{m!} \frac{d^m F(\tilde{x})}{d\tilde{x}^m} \left(\frac{\tilde{x}_{n+k} + \tilde{x}_{n+k+1}}{2} - \tilde{x}\right)^m \; . \tag{16}$$

Now we expand

$$\tilde{x}_{n+k} = \tilde{x} + \sum_{m=1}^{\infty} \phi_{km} \alpha^{-m} \; , \tag{17}$$

and insert the expansion into Eq. (16). By requiring all orders of α^{-1} to cancel, the coefficients ϕ_{km} are found for any values of k and m. These coefficients involve the function F and its derivatives evaluated at $\tilde{x} = (\tilde{x}_n + \tilde{x}_{n+1})/2$.

We now return to Eq. (14). It depends on the velocities $\dot{\tilde{x}}_n$ and $\dot{\tilde{x}}_{n+1}$, which in turn depend on $\tilde{x}_{n-2}, \ldots, \tilde{x}_{n+3}$. Using Eq. (17) we expand Eq. (14) in α^{-1}. The result of this expansion in the general NDL case is

$$\frac{3}{4}\cdot\frac{d^2}{d\tilde{x}^2}\left(\frac{1}{F}\cdot\frac{d^2F^2}{d\tilde{x}^2}\right)+\frac{\dot{\alpha}}{\alpha}\cdot F+\mathcal{O}\left(\alpha^{-2}\right)=0\ . \tag{18}$$

In the DL case the expansion result is different:

$$\frac{3}{2}\cdot\frac{d^4F^2}{d\tilde{x}^4}+\frac{\dot{\alpha}}{\alpha^2}\cdot F+\mathcal{O}\left(\alpha^{-2}\right)=0\ . \tag{19}$$

Consider Eq. (18) in the scaling limit, $\alpha\to\infty$. The α^{-2} term can be ignored and we are left with the first two terms, which must cancel each other. This implies that $\dot{\alpha}/\alpha$ is independent of time, i.e., in the NDL case

$$\alpha\propto e^{-\tilde{t}/\tau_{NDL}}\ , \tag{20}$$

where τ_{NDL} is the life time of the profile. Note that the scaling limit $\alpha\to\infty$ corresponds to very early times $\tilde{t}\to-\infty$. The equation for the NDL scaling function in this limit is

$$\frac{3}{4}\cdot\frac{d^2}{d\tilde{x}^2}\left(\frac{1}{F}\cdot\frac{d^2F^2}{d\tilde{x}^2}\right)-\frac{F}{\tau_{NDL}}=0\ . \tag{21}$$

At any finite time when α itself is finite, there will be a correction to scaling of order α^{-2}.

The same arguments can be applied to Eq. (19) in the DL case. We find that $\dot{\alpha}/\alpha^2$ is independent of time, i.e.,

$$\alpha=\frac{\tau_{DL}}{\tilde{t}-\tilde{t}_0}\ . \tag{22}$$

In this case the scaling limit corresponds to a *finite* time, $\tilde{t}\to\tilde{t}_0^+$. The differential equation for the DL case is

$$\frac{3}{2}\cdot\frac{d^4F^2}{d\tilde{x}^4}-\frac{F}{\tau_{DL}}=0\ . \tag{23}$$

Again there is a correction to scaling of order α^{-2} when $t>t_0$.

Note that the scaling equation is the same for all NDL cases. Thus, for all non-zero values of $l=\frac{2D_s}{k}$, the scaling behavior is identical to that of the ADL limit. Since in the NDL case the terrace sizes vanish in the scaling limit, diffusion across terraces is fast and, unless the system if purely DL ($l=0$), attachment-detachment is always the rate limiting process. This fact makes the DL case special and somewhat delicate. Since in real systems the diffusion coefficient is always finite, the scaling limit of real systems will show ADL behavior. Nevertheless, at finite times we can expect crossover from ADL to DL behavior. This should happen at the time when $\frac{1}{\alpha F}\approx l$. At later times, when $\frac{1}{\alpha F}\gg l$, the system should show DL behavior and obey Eq. (23), provided α is still large enough to neglect the α^{-2} corrections to scaling.

At this point we have a continuum model derived directly from the discrete step equations of motion. In the scaling limit our model provides an exact connection between the microscopic step kinetics and the macroscopic surface evolution. It is interesting to compare it with other continuum models, which do not emerge from the underlying step model.

In the usual continuum approach one assumes that surface dynamics is driven by the surface tendency to decrease its *continuous* surface tension. Below the roughening transition this surface tension has a cusp and takes the form[8,27]

$$\sigma(D)=\sigma_0+\sigma_1|D|+\sigma_3|D|^3\ , \tag{24}$$

with D denoting the surface slope. The surface chemical potential is consequently given by

$$\mu = \frac{\partial \sigma'(D)}{\partial x} \ , \tag{25}$$

where σ' is the derivative of σ with respect to the slope D. This chemical potential gives rise to surface currents, which are proportional to $\partial\mu/\partial x$ in the DL case[7,16,27] and to $\partial\mu/\partial h = \frac{1}{D}\frac{\partial\mu}{\partial x}$ in the ADL case[27]. The equation of motion for the profile slope in regions where $D > 0$ is then given by

$$\frac{\partial D}{\partial t} \propto -3\sigma_3 \frac{\partial^2}{\partial x^2}\left(\frac{1}{D}\frac{\partial^2 D^2}{\partial x^2}\right) \tag{26}$$

in the ADL case, and

$$\frac{\partial D}{\partial t} \propto -3\sigma_3 \frac{\partial^4 D^2}{\partial x^4} \tag{27}$$

in the DL case.

To compare our model with the above equations, let us find the general equation of motion for the density function; i.e., the partial differential equation for the step density that by separation of variables, $D(\tilde{x},\tilde{t}) = \alpha(\tilde{t})F(\tilde{x})$, reduces to Eqs. (20) & (21) in the NDL case and to Eqs. (22) & (23) in the DL case. In the NDL case we can replace τ_{NDL} in Eq. (21) by $-\dot{\alpha}/\alpha$. The equation can then be written as

$$\frac{3}{4}\cdot\frac{\partial^2}{\partial\tilde{x}^2}\left(\frac{1}{D}\cdot\frac{\partial^2 D^2}{\partial\tilde{x}^2}\right) + \frac{\partial D}{\partial\tilde{t}} = 0 \ , \tag{28}$$

which is consistent with Eq. (26) and confirms Nozieres' suggestion[27] for ADL kinetics. Note that Eq. (28) applies only to ADL cases and not to the full range of NDL systems, because in the scaling limit all NDL systems obey Eq. (21), which describes ADL kinetics. Since Eq. (28) was derived from Eq. (21) it corresponds to ADL kinetics.

For the DL case we replace τ_{DL} in Eq. (23) by $-\dot{\alpha}/\alpha^2$. We then have

$$\frac{3}{2}\cdot\frac{\partial^4 D^2}{\partial\tilde{x}^4} + \frac{\partial D}{\partial\tilde{t}} = 0 \ , \tag{29}$$

consistently with Eq. (27) and Refs. 7,16 and 27. Let us however remark that the validity of the general Eqs. (28) and(29) is questionable. In a non scaling case these equations have corrections which may be important. We showed that in the scaling state these corrections vanish and neglected them in moving from Eqs. (18) & (19) to (21) & (23). In a general scenario, neglecting these terms is an approximation that must be justified.

IV. SOLUTION OF THE CONTINUUM MODELS

In this section we find the scaling functions in the NDL and DL cases. Since the slope-up and slope-down sections are symmetric, we need to consider only half a period, i.e., the section $\tilde{x} \in [-\pi/2, \pi/2]$. The scaling function is thus symmetric about the origin.

We now discuss the possibility of macroscopic facets at the profile extrema. In terms of the discrete step model every terrace is a facet. However, in the scaling limit the step density diverges with $\alpha(\tilde{t})$, and the terraces in all regions where F is finite become truly microscopic. In regions where the scaling function is identically zero the terrace size does

not necessarily vanish and macroscopic facets may form. To account for macroscopic facets we should, in principle, allow for regions of arbitrary size with $F = 0$. However, simulations of the discrete step model indicate that if such regions appear at all, they form around the profile extrema where the step density is zero by definition. To account for macroscopic facets, we therefore allow for the existence of two special points at $\pm\tilde{x}_{facet}$, which denote the positions of facet edges. In the regions $(-\pi/2, -\tilde{x}_{facet})$ and $(\tilde{x}_{facet}, \pi/2)$ the scaling function F vanishes identically. In this notation we can also describe systems without facets simply by setting $\tilde{x}_{facet} = \pi/2$. Note that the scaling function should satisfy Eq. (21) or (23) only in the interval $(-\tilde{x}_{facet}, \tilde{x}_{facet})$ and not on the facet, since these equations are not valid when $F = 0$.

Next we show that if there is a macroscopic facet, F is continuous across the facet edge. To see this, consider the annihilation process of the first step. Its velocity satisfies

$$\dot{\tilde{x}}_1 \propto \frac{(\tilde{x}_3 - \tilde{x}_2)^{-3} - 2(\tilde{x}_2 - \tilde{x}_1)^{-3} - g(\tilde{x}_1 - \tilde{x}_0)^{-3}}{\frac{2\pi l}{\lambda} + \tilde{x}_2 - \tilde{x}_1} \ . \tag{30}$$

The denominator in the above expression is always positive. Therefore the direction of motion of the first step is given by the sign of the numerator, which must be negative because the first step is moving towards annihilation with the zeroth step. Assume now that in the scaling limit we have a macroscopic facet. This means that the distance $\tilde{x}_1 - \tilde{x}_0$ is finite when the annihilation process starts. Assume also that $F_{facet} = F(\tilde{x}_{facet})$ is finite. This makes the distance $\tilde{x}_3 - \tilde{x}_2$ microscopically small, since in the scaling limit it vanishes as $1/(\alpha F_{facet})$. We can therefore neglect the last term in the numerator of Eq. (30). It is easy to see now that if $\tilde{x}_2 - \tilde{x}_1 < 2^{1/3}/(\alpha F_{facet})$ the velocity of the first step is positive. Thus if F_{facet} is finite, the first step is bounded to the second one at a distance which is much less than the facet size. In such a situation the first step cannot annihilate. We conclude that having a macroscopic facet ($\tilde{x}_{facet} < \pi/2$) requires the scaling function to vanish at the facet edge. Thus the scaling function is continuous at $\tilde{x}_{facet}$ with $F(\tilde{x}_{facet}) = 0$. Furthermore, by expanding the scaling function in the vicinity of $\tilde{x}_{facet}$, it can be shown that both the NDL and DL scaling functions can be expressed as power series of $\sqrt{\tilde{x}_{facet} - \tilde{x}}$:

$$F(\tilde{x}) = \sum_{n=1}^{\infty} a_n \left(\sqrt{\tilde{x}_{facet} - \tilde{x}}\right)^n \ . \tag{31}$$

Hence with a non-vanishing coefficient a_1, the derivatives of the scaling function diverge at $\tilde{x}_{facet}$.

Next we specify boundary conditions for the scaling function F. Since Eqs. (21) and (23) are fourth order differential equations we need four boundary conditions in order to solve them. Three conditions are set by the normalization and symmetry of the scaling function:

$$\begin{aligned} &F(0) = 1 \ , \\ &F'(0) = 0 \ , \\ &F'''(0) = 0 \ . \end{aligned} \tag{32}$$

A fourth boundary condition can be found by considering mass transfer in the decaying profile. Mass is transfered from the decaying peaks to the valleys through the sloping parts of the profile. The step-antistep symmetry of the system excludes mass transfer through the profile extrema. We can thus calculate the (dimensionless) flux through the origin by calculating the (dimensionless) volume change in the interval $[0, \pi/2]$:

$$J(0) = \frac{d}{d\tilde{t}} \int_0^{\pi/2} h(\tilde{x}, \tilde{t}) d\tilde{x} \ . \tag{33}$$

$h(\tilde{x},\tilde{t})$ is the surface profile measured in steps. In the continuum limit it is given by

$$h(\tilde{x},\tilde{t}) = \int_0^{\tilde{x}} D(\xi,\tilde{t})d\xi \ . \tag{34}$$

Integrating Eq. (33) by parts and using the scaling form (12) together with the possible existence of zero density facets results in

$$J(0) = \dot{\alpha} \int_0^{\tilde{x}_{facet}} F \cdot (\pi/2 - \tilde{x})\, d\tilde{x} \ . \tag{35}$$

To evaluate the integral in Eq. (35) in the NDL case, we multiply Eq. (21) by $(\pi/2 - \tilde{x})$ and integrate from zero to $\tilde{x}_{facet}$:

$$\int_0^{\tilde{x}_{facet}} F \cdot (\pi/2 - \tilde{x})\, d\tilde{x} = \frac{3\tau_{NDL}}{4} \cdot \int_0^{\tilde{x}_{facet}} (\pi/2 - \tilde{x})\, \frac{d^2}{d\tilde{x}^2} \cdot \left(\frac{1}{F} \cdot \frac{d^2F^2}{d\tilde{x}^2} \right) d\tilde{x} \ . \tag{36}$$

The r.h.s. of the last equation can be integrated by parts. Inserting the result into Eq. (35) we find that

$$J(0) = \frac{3\tau_{NDL}\dot{\alpha}}{4} \left[(\pi/2 - \tilde{x})\, \frac{d}{d\tilde{x}} \left(\frac{1}{F} \cdot \frac{d^2F^2}{d\tilde{x}^2} \right) + \frac{1}{F} \cdot \frac{d^2F^2}{d\tilde{x}^2} \right] \Bigg|_0^{\tilde{x}_{facet}} \ . \tag{37}$$

Another method for calculating the flux through the origin relies on the discrete step system. The adatom flux across the nth terrace is given by Eq. (3), which can be expanded in powers of α^{-1} using Eq. (17). In our dimensionless variables, the leading order of this expansion in the NDL case is

$$J(\tilde{x}) = \frac{3\alpha}{4F} \cdot \frac{d^2F^2}{d\tilde{x}^2} \ . \tag{38}$$

Evaluating this expression at $\tilde{x} = 0$ and comparing with Eq. (37), we obtain the boundary condition

$$\left[(\pi/2 - \tilde{x}) \cdot \frac{d}{d\tilde{x}} \left(\frac{1}{F} \cdot \frac{d^2F^2}{d\tilde{x}^2} \right) + \frac{1}{F} \cdot \frac{d^2F^2}{d\tilde{x}^2} \right] \Bigg|_{\tilde{x}_{facet}} = 0 \ . \tag{39}$$

In deriving this boundary condition we used the fact that $F'(0) = F'''(0) = 0$ and that in the NDL case $\tau_{NDL} = -\alpha/\dot{\alpha}$.

The DL case is very similar. We can evaluate the flux through the origin both from Eq. (35) and from a direct expansion of Eq. (3). Equating the two results we obtain the fourth boundary condition in the DL case

$$\left[(\pi/2 - \tilde{x}) \cdot \frac{d^3F^2}{d\tilde{x}^3} + \frac{d^2F^2}{d\tilde{x}^2} \right] \Bigg|_{\tilde{x}_{facet}} = 0 \ . \tag{40}$$

At this point we have four boundary conditions for the scaling function, three at the origin and one at $\tilde{x}_{facet}$. In addition we know that $F(\tilde{x}_{facet}) = 0$ if $\tilde{x}_{facet} < \pi/2$. We may now find unique scaling solutions if we know the values of τ_{NDL} and τ_{DL}, which enter in the differential equations (21) and (23). What determines the values of τ_{NDL} and τ_{DL}? We now show that these life times are related to the behavior of the top and bottom steps, which are unique in the sense that they each have a neighboring step of opposite sign. Our continuum

model, which treats all steps on equal footing, does not contain any information about this unique behavior and therefore τ_{NDL} and τ_{DL} must be calculated or measured directly from the discrete step system.

To relate the profile life times to the behavior of the top and bottom steps, consider the number of steps in a half slope up region of the profile. One can show from Eq. (34) that it is given by

$$N(t) = \int_0^{\pi/2} D(\tilde{x},\tilde{t})d\tilde{x} = \alpha \int_0^{\tilde{x}_{facet}} F d\tilde{x} \ . \tag{41}$$

The integral $\mathcal{I} = \int_0^{\tilde{x}_{facet}} F d\tilde{x}$ can be evaluated by integrating Eqs. (21) or (23) in the NDL or the DL cases, respectively. The results are

$$\begin{aligned} \mathcal{I}_{NDL} &= \frac{3\tau_{NDL}}{4}\frac{d}{d\tilde{x}}\left(\frac{1}{F}\cdot\frac{d^2F^2}{d\tilde{x}^2}\right)\Bigg|_{\tilde{x}_{facet}} \ , \\ \mathcal{I}_{DL} &= \frac{3\tau_{DL}}{2}\frac{d^3F^2}{d\tilde{x}^3}\Bigg|_{\tilde{x}_{facet}} \ . \end{aligned} \tag{42}$$

Combining Eqs. (41) and (42) we can calculate $\Delta\tilde{t}$, the time interval in which the system looses one step, i.e., the annihilation time of the top step:

$$\Delta\tilde{t} = \frac{d\tilde{t}}{dN} = \frac{1}{\dot{\alpha}\mathcal{I}} \ . \tag{43}$$

Eq. (43) relates the profile decay rate, α, to the annihilation time of a single step at the profile peak, $\Delta\tilde{t}$. We could have used this relation to set an additional condition at $\tilde{x}_{facet}$ if we knew $\Delta\tilde{t}$. Such a condition would select a single solution with a specific life time from the one dimensional family of possible solutions. However, as we mentioned above, $\Delta\tilde{t}$ must be obtained directly from the discrete system, because our continuum model ignores the unique behavior of the top step.

Unable to calculate the life times of the profiles analytically, we measured τ_{NDL} and τ_{DL} from our simulations. Using these values we solved Eqs. (21) and (23) numerically. In Fig. 5 we show the results for a single slope-up region of the profile in the ADL case and compare them with the simulation data. The slope-down regions of the profile behave in exactly the same way, but with a negative step density (to be consistent with the profile slope). In the insets we show the surface profile, which is obtained by integrating the scaling function over alternating regions of steps and antisteps. Similar results were obtained in the DL case.

The following picture emerges. Both in the ADL and DL cases, when step-antistep attraction is absent ($g = 0$) the unique scaling solutions, which satisfy all the boundary conditions, have no facets. The scaling functions obey Eqs. (21) and (23) in the entire interval $(-\pi/2, \pi/2)$ and are finite at the profile extrema ($\tilde{x} = \pm\pi/2$). This results in cusp-like peaks and valleys in the surface profile. The agreement between the scaling functions and the simulation data is excellent in these cases. When step-antistep attraction is present ($g = 24$) the situation is different. The unique scaling solutions, which satisfy all the boundary conditions, have small facets near the profile extrema. In the facet region the scaling functions are identically zero and as a result the profiles have flat peaks and valleys. Here we also have good agreement with simulation data, but not as good as in the $g = 0$ cases. This is because the scaling ansatz is a better approximation when $g = 0$.

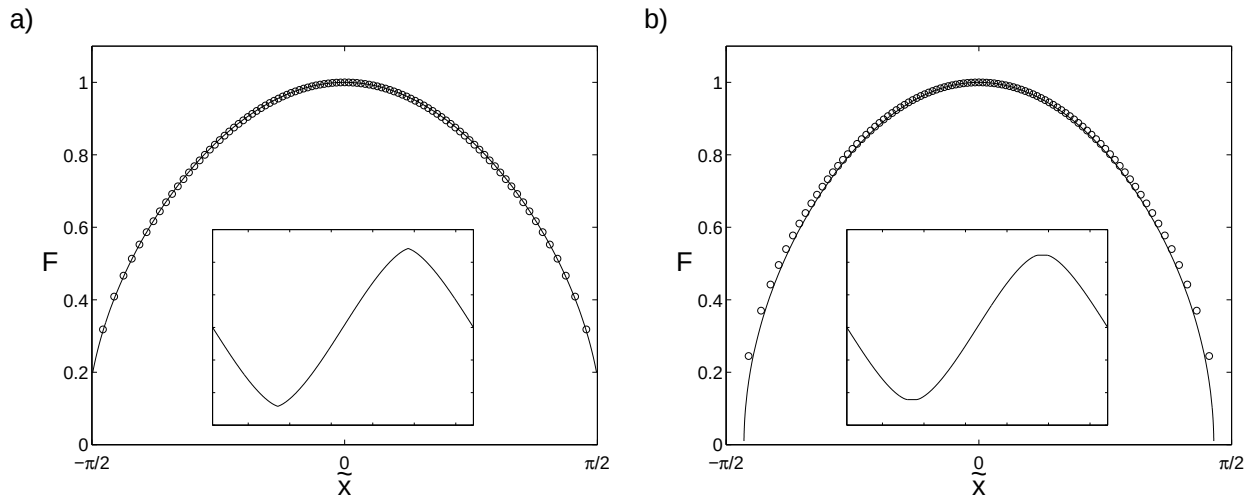

FIG. 5. Scaling function solutions (solid) compared with simulation data (circles) in the ADL case. Only a single slope up region is shown. The insets show the resulting surface profiles obtained by integrating the scaling functions over alternating regions of steps and antisteps with a) $g = 0$ and b) $g = 24$.

V. CONNECTION WITH EXPERIMENT

In this section we test our model against experimental results. Specifically we compare our predictions with AFM measurements carried out by Tanaka et al[3]. They measured the amplitude of decaying 1D Silicon gratings fabricated on a surface vicinal to the Si(001) plane. They report an exponential decay of the surface amplitude with life times scaling as the fourth power of the grating wavelength. The observed profiles had flat peaks and valleys. These results qualitatively resemble the behavior of our model in the NDL case in the presence of step-antistep attraction.

To prepare the ground for a more quantitative comparison, let us first discuss the relevance of our model to the experimental system. The experimental conditions where such that the Si surface was below its roughening transition. It is therefore reasonable to expect step-dominated surface kinetics. However, the step structure in the experiment is different from the idealized one dimensional array of straight steps we considered in our model. Since the grating was fabricated on a vicinal surface, with the grooves direction perpendicular to the unperturbed steps, the steps are not straight. This can be easily shown by writing the surface profile as

$$Z(x, y) = h(x) + ay \ . \tag{44}$$

Here $h(x)$ is the one dimensional periodic profile along the x axis and $Z(x, y)$ is the two dimensional surface profile. The parameter a measures the slope of the original vicinal surface with respect to the high symmetry (x, y) plane. The constant height contours which define the steps are given by

$$y_n(x) = \frac{Z_n - h(x)}{a} \ . \tag{45}$$

Evidently, we deal here with curved steps, a fact which complicates surface dynamics. This situation was studied by Bonzel and Mullins[28] who investigated the smoothing of perturbed vicinal surfaces. In addition to step-step interactions, step motion is also driven by the steps line tension, Γ. This is reflected by the addition of a term $\mu_n^{curv}(x) = \Gamma/R_n(x)$ to the step chemical potential, where $R_n(x)$ is the local radius of curvature of the nth step.

The above arguments suggest that our straight steps model cannot describe surface dynamics in regions where line tension is important. To justify the application of our model to the experimental system we must therefore show that we can neglect the effect of step line tension. We do this by considering the scaling limit of the system. We show that in this limit the steps in the sloping parts of the profile are effectively straight. The only regions where step curvature is significant are the profile extrema, where our continuum model is not valid anyway. Unlike Bonzel and Mullins we consider situations where step curvature is a driving force for step straightening only at the profile extrema.

Assume now that the step system (45) exhibits scaling and obeys Eq. (12). $D(x,t) = dh/dx$ is the step density along the x axis. Under these assumptions we can express the step curvature contribution to the chemical potential as

$$\mu_n^{curv}(x) = \frac{\Gamma y_n''}{\left[1+(y_n')^2\right]^{3/2}} = -\frac{\Gamma\alpha F'}{a\left(1+\frac{\alpha^2F^2}{a^2}\right)^{3/2}} \ , \tag{46}$$

with primes denoting derivatives with respect to x. Note that according to Eq. (46), $\mu_n^{curv}(x) \equiv \mu^{curv}(x)$ is independent of n.

Let us estimate the effect of $\mu^{curv}(x)$ on step kinetics. This chemical potential gives rise to surface currents parallel and perpendicular to the steps. The divergence of these currents contributes to the step velocities. Along a step we can estimate the resulting current as $J_\parallel \propto d\mu^{curv}(x)/ds$ where s is the step arclength. The contribution of this current to the step velocity is proportional to

$$\frac{d^2\mu^{curv}(x)}{ds^2} = \frac{\Gamma\left(-\frac{\alpha F'''}{a}+\frac{\alpha^3\left(3F'^3+10FF'F''-2F^2F'''\right)}{a^3}+\frac{\alpha^5\left(-15F^2F'^3+10F^3F'F''-F^4F'''\right)}{a^5}\right)}{\left(1+\frac{\alpha^2F^2}{a^2}\right)^{9/2}} \ . \tag{47}$$

In the scaling limit $\alpha\to\infty$, this contribution decays as α^{-4} wherever F is finite. This result should be compared with the step velocities of the original model. Using the expansion Eq. (17), we can expand the original step velocities, Eq. (4), in α^{-1}. The outcome of this manipulation is a velocity of order 1. Thus, in the scaling limit, the curvature driven current along the steps results in a negligible contribution to the step velocities.

The current perpendicular to a step is proportional to the chemical potential difference between two adjacent steps. This can be estimated from $J_\perp \propto \hat{n}\cdot\nabla\mu^{curv}(x)/|\nabla Z|$ where $\hat{n}$ is a unit vector perpendicular to the step. However, since we are only interested here in the leading order in α^{-1}, we can make the approximation $\hat{n}\approx x$, $|\nabla Z|\approx\alpha F$ and $J_\perp \propto \frac{1}{\alpha F}\frac{d\mu^{curv}(x)}{dx}$ wherever F does not vanish. The contribution of these currents to the step velocity is consequently proportional to the current difference between two adjacent terraces which we estimate as

$$\frac{1}{\alpha F}\frac{d}{dx}\left(\frac{1}{\alpha F}\frac{d\mu^{curv}(x)}{dx}\right) = -\frac{\Gamma\alpha^{-4}a^2\left(15F'^3-10FF'F''+F^2F'''\right)}{F^7}+\mathcal{O}\left(\alpha^{-6}\right) \ . \tag{48}$$

Again this contribution in negligible in the scaling limit.

The above argument relies on the fact that in the sloping parts of the profile F is finite. This is of course not true near the profile extrema. Step curvature is therefore important at the facets near the profile peaks and valleys where the scaling function F is identically zero. Thus, we can divide the system into two types of regions: the sloping parts where our continuum model is valid and the facets where our continuum model breaks down. Recall however that our model breaks down on facets in any case, and we solve the model only on

the sloping parts of the profile. The kinetics of the annihilating steps on the facets enters the continuum model only through the life time of the profile, which we have to take from the discrete step system. We can use this strategy here, i.e., by measuring the life time of the profile from the experimental results we can predict (using Eq. (21)) the density scaling function. Alternatively, by fitting the scaling function to the experiment we can make a connection between the experimental life time τ_{exp}, and the microscopic parameters of the system. In Fig. 6 we show a comparison between a snapshot of the normalized experimental slope and the best fit solution of Eq. (21). This solution corresponds to a life time $\tau_{NDL} = 0.945$ in dimensionless units. According to Eq. (10) the three microscopic parameters k, $\tilde{C}^{eq}$ and β satisfy

$$k\tilde{C}^{eq}\beta = \left(\frac{\lambda}{2\pi}\right)^4 \frac{k_B T \tau_{NDL}}{\Omega \tau_{exp}} \ . \tag{49}$$

The parameter values for the experimental data of Fig. 6 are $\lambda = 5\ \mu m$, $\tau_{exp} \approx 2.4 \cdot 10^3$ minutes and $T = 900°C$.

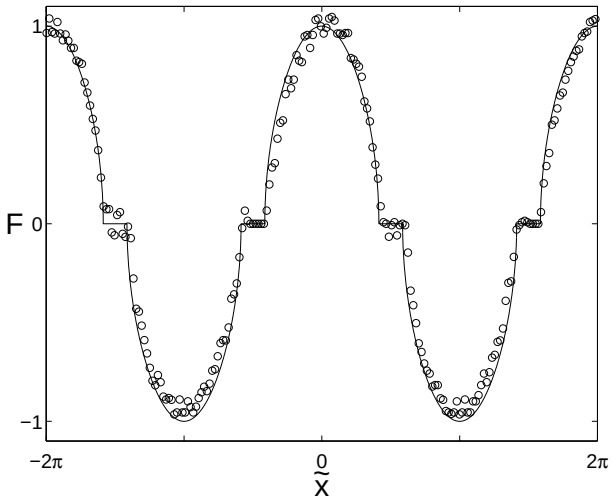

FIG. 6. Comparison between a snapshot of the experimental slope and the best fit solution of Eq. (21). This solution corresponds to a life time $\tau_{NDL} = 0.945$. The experimental slope was normalized to a 2π wavelength and unit maximal slope.

Although Fig. 6 shows good agreement between theory and experiment it does not by itself provide enough evidence for scaling in the experimental system. To verify that the experimental system scales in time one must analyze several snapshots of the surface slope taken at different times. However, the fit quality and the fact that the surface amplitude decays exponentially with a life time proportional to the fourth power of the grating wavelength, strongly suggest scaling.

VI. SUMMARY AND DISCUSSION

In this work we have studied the relaxation process of one dimensional surface modulations below the roughening transition temperature. Simulations of a step flow model suggest that the *discrete* step density function, $D(x,t)$, exhibits scaling throughout most of the decay process, for a wide range of the model parameters, spanning DL to ADL kinetics and a range of strengths of the attraction between steps of opposite sign.

Relying on the above observations, we then transformed the discrete step model into a continuum model for surface dynamics. This was done using the scaling ansatz $D(x,t) = \alpha(t)F(x)$, and we were able to write down the differential equations for the functions $\alpha(t)$

and $F(x)$. These equations were derived directly from the discrete step equations of motion. We showed that they are exact in the scaling limit.

We investigated the boundary conditions for the scaling function F and found F numerically. A comparison between the resulting solutions and density functions from simulations of the discrete step model shows impressive agreement.

Finally, we applied our continuum model to experimental data measured by Tanaka et al[3]. They reported exponential amplitude decay of Si(001) gratings and profiles with flat peaks and valleys. In their experiment the profile life times scaled as the fourth power of the grating wavelength. These properties resemble the behavior of our model in the NDL case with step-antistep attraction. We showed that in the scaling limit, our one dimensional model is adequate in spite of the fact that the steps in the experimental system are not straight. We compared the best fit solution of our model to a normalized snapshot of the experimental profile slope and found good agreement. On the basis of this agreement we suggested that the profile exhibits scaling and made a connection between the measured profile life time and microscopic system parameters.

We now discuss the main aspects of our results and put them in perspective with existing work. In the scaling limit our continuum model is an exact result of step kinetics. We showed that the resulting general differential equations ((28) and (29)) are equivalent to existing phenomenological models[7,16,27], thereby confirming that these models are consistent with step flow. Although we have not discussed this issue here, it can be shown that the scaling solutions $D(x,t) = \alpha(t)F(x)$ are linearly stable solutions of the general differential equations ((28) and (29)). This fact may explain why scaling solutions are selected. However, our analysis shows that these differential equations have corrections which originate from the discrete nature of the system. When these corrections are important, one must take into account the full expansion series (17). This results in differential equations of infinite order. Therefore Eqs. (28) & (29) and other equivalent models are valid only in situations where corrections can be ignored. We proved that the scaling scenario is such a case by showing how these corrections vanish in the scaling limit.

The second point we emphasize is that even in a scaling limit there are regions where the discrete nature of steps becomes important. Such regions are the profile extrema where step-antistep pairs annihilate. The reason for this is twofold. First, the steps near the profile extrema are unique in the sense that they have a neighboring step of opposite sign. They therefore follow unique equations of motion. This does not enter in our continuum model which treats all steps on equal footing. Secondly, our continuum model breaks down near zeros of the scaling function. This can be seen in the derivation of the model, which relies on F being finite. The kinetics of steps in regions where the step density vanishes are not described by the model, since corrections to the scaling function become important there. In cases where the profile extrema are faceted, our continuum model cannot account for the kinetics of steps on the facets even if these steps follow the general discrete equations of motion.

It is therefore obvious that our continuum model (and all other equivalent differential equations) does not constitute a complete description of surface evolution. A manifestation of this statement is the fact that the relative attraction strength, g, is not a parameter of the continuum model, even though it strongly affects surface evolution. Since our continuum model breaks down near the profile extrema, their effect must be taken into account by supplying additional information. In our case, this information is the value of the profile life time. As we showed in section IV, this life time determines the annihilation rate of step-antistep pairs and can be considered as the last boundary condition required for finding the scaling function. Thus, in a scaling scenario, the effect of step kinetics near the profile extrema reduces to a boundary condition for the scaling function at $\pm\tilde{x}_{facet}$. In order to solve for F consistently with the discrete model, it is sufficient to supply the profile life time. We did this by measuring the life times of the discrete systems.

In this respect our work is different from other continuum treatments of modulated surfaces. As pointed out by Chame et al[19], lack of consistency with the kinetics of facet steps is the weakness of existing continuum models. One remarkable outcome of these inconsisten-

cies is the controversy regarding the appearance of facets at the profile extrema. Ozdemir & Zangwill[7] and Hager & Spohn[16] both used continuum models, which are equivalent to Eq. (29). Bonzel and Preuss[18] use a slightly different model in which the surface currents are proportional to the derivative of the chemical potential with respect to the surface arclength. But they all start from a continuum approach and do not specify the step kinetics on the facets.

Ozdemir and Zangwill assume that Eq. (29) is valid in the full interval between the profile extrema and thus exclude the possibility of facet formation. Their results show smooth (but nonanalytic) profiles. This corresponds to some weak attractive step-antistep interaction (in the absence of such interaction we get cusped profiles). They showed that Eq. (29) admits shape preserving solutions, equivalent to our scaling solutions in the DL case. In particular they showed that the amplitude α of a shape preserving profile obeys Eq. (22). Our results for the decay rate in the DL case are mathematically identical, but we interpret them differently. While Ozdemir and Zangwill look at the long time limit in which $\alpha \sim t^{-1}$, we recognize that Eq. (29) is valid only in the scaling limit, where $t \gtrsim t_0$. In this case $\alpha \not\sim t^{-1}$.

Hager and Spohn, on the other hand, allow for facet formation by solving Eq. (29) with moving boundaries. They assume that the chemical potential, the current and the current divergence are all continuous at the facet edge. In their model, the chemical potential at the facet edge is not a step chemical potential. It is a *layer* chemical potential which reflects the free energy change caused by the annihilation of the top step-antistep pair. In this way they allow for the top terraces to peel rapidly. Their model produces facets which grow in time.

Our results are different. First, since we start from step flow, the chemical potential in our continuum model is a *step* chemical potential. On a facet our chemical potential is not defined (and therefore not continuous) since there are no steps there. One can argue that the adatom chemical potential on the facet is equal to the chemical potential of the top first step. But this first step is unique and is not treated by the continuum model. It is also far from equilibrium with its neighbors so there is no reason to assume continuity of the chemical potential. Second, the appearance of facets in our model depends on strength of the step-antistep attraction.

Bonzel and Preuss deal with facets differently. They round the cusp singularity of the surface tension, Eq. (24), and apply the kinetic surface equation everywhere. They thus obtain analytic profiles with very flat extrema but without actual faceting. Again the weakness of this approach is that it is not clear how this rounding is related to the microscopic behavior of steps.

We conclude that our continuum model is fully consistent with step kinetics, but is restricted to scaling scenarios. It may serve both as a starting point and a test case, for new continuum models which will attempt to describe surface evolution in general and facet kinetics in particular.

We are greatful to C. C. Umbach for supplying the experimental data and for helpful discussions. This research was supported by grant No. 95-00268 from the United States-Israel Binational Science Foundation (BSF), Jerusalem, Israel.

---

* E-mail: israeli@wicc.weizmann.ac.il
** E-mail: daniel.kandel@weizmann.ac.il, http://www.weizmann.ac.il/∼fekandel.

[1] K. Yamashita, H. P. Bonzel and H. Ibach, Appl. Phys. **25**, 231 (1981);

[2] W. W. Mullins, J. Appl. Phys. **28**, 333 (1957); **30**, 77 (1959).

[3] S. Tanaka, C. C. Umbach, J. M. Blakely, R. M. Tromp and M. Mankos, J. Vac. Sci. Technol. A **15(3)** 1345 (1997).

[4] S. Tanaka, C. C. Umbach, J. M. Blakely, R. M. Tromp and M. Mankos, Mat. Res. Soc. Symp. Proc. **440** 25 (1997).
[5] J. Blakely, C. Umbach and S. Tanaka, Dynamics of Crystal Surfaces and Interfaces, edited by P. M. Duxbury and T. J. Pence (Plenum, New York, 1997), p. 23.
[6] C. C. Umbach, M. E. Keeffe and J. M. Blakely, J. Vac. Sci. Technol. A **9**, 1014 (1991).
[7] M. Ozdemir and A. Zangwill, Phys. Rev. B **42**, 5013 (1990).
[8] A. Rettori and J. Villain, J. Phys. France **49**, 257 (1988).
[9] C. Duport, A. Chame, W. W. Mullins and J. Villain, J. Phys. I France **6**, 1095 (1996).
[10] M. V. Ramana Murty and B. H. Cooper, Phys. Rev. B **54**, 10377 (1996). These Monte Carlo simulations agree with[8,7].
[11] E. Adam, A. Chame, F. Lancon and J. Villain, J. Phys. I France **7**, 1455 (1997).
[12] M. A. Dubson and G. Jeffers, Phys. Rev. B **49**, 8347 (1994).
[13] Z. Jiang and C. Ebner, Phys. Rev. B **40**, 316 (1989).
[14] W. Selke and P. M. Duxbury, Phys. Rev. B **52**, 17468 (1995).
[15] J. D. Erlebacher and M. J. Aziz, Surf. Sci. **374**, 427 (1997).
[16] J. Hager and H. Spohn, Surf. Sci. **324**, 365 (1995).
[17] H. P. Bonzel, E. Preuss and B steffen, Appl. Phys. A **35**, 1 (1984).
[18] H. P. Bonzel and E. Preuss, Surf. Sci. **336**, 209 (1995).
[19] A. Chame, S. Rousset, H. P. Bonzel and J. Villain, Bul. Chem. Comm. **29**, 398 (1996/1997).
[20] N. Israeli and D. Kandel, Phys. Rev. Lett. **80** 3300 (1998).
[21] N. Israeli and D. Kandel, Phys. Rev. B **60** 5946 (1999).
[22] N. Israeli, H-C. Jeong, D. Kandel and J. D. Weeks, Phys. Rev. B **61** 5698 (2000).
[23] W. K. Burton, N. Cabrera and F. C. Frank, Philos. Trans. R. Soc. London, Ser. A **243**, 299 (1951).
[24] G. S. Bales and A. Zangwill, Phys. Rev. B **41** 5500 (1990).
[25] V. I. Marchenko and A. Ya. Parshin, Zh. Eksp. Teor. Fiz. **79**, 257 (1980) [Sov. Phys. JETP **52**, 129 (1980)].
[26] A. F. Andreev and Yu. A. Kosevich, Zh. Eksp. Teor. Fiz. **82**, 1435 (1981) [Sov. Phys. JETP **54**, 761 (1982)].
[27] P. Nozieres, J. Phys. I France **48**, 1605 (1987).
[28] H. P. Bonzel and W. W. Mullins, Surf. Sci. **350**, 285 (1996).
[29] F. Lancon and J. Villain, Phys. Rev. Lett. **64**, 293 (1990).